BY-NC

Marek St. Węglowski, Robert Jachym, Krzysztof Krasnowski, Krzysztof Kwieciński, Janusz Pikuła, Piotr Śliwiński

Electron Beam Melting of Thermally Sprayed Layers – Overview

Abstract: Thermal spraying is one of the most common methods enabling the deposition of variously-purposed layers on surfaces of structural elements. However, in certain cases, the process of spraying itself is ineffective in terms of the stability and properties of protective layers. One of the possible solutions making it possible to reduce the porosity and improve the adhesion of surfaced layers involves their melting using the concentrated electron beam. The article contains an overview of reference publications concerning electron beam melting technologies.

Keywords: thermal spraying, melting, electron beam

DOI: *10.17729/ebis.2021.3/1*

Introduction

Thermal spraying technologies enable the making of layers using a wide range of metallic, ceramic and plastic-based materials. Significant demand for thermally sprayed layers is best illustrated by the market worth, which amounted to 7.6 billion \$ in 2020 and is expected to reach 10.7 billion \$ in 2025 (with an accumulated annual growth of 7.0%) [1]. Thermally sprayed layers find applications primarily in the aviation and automotive industries as well in medicine, production of turbines and the making of special-purpose structures (e.g. exposed to abrasive wear, high operating temperature or a corrosive environment).

An important advantage of spraying technologies is the slight heating of the base material during layer deposition, limiting microstructural transformations and substrate deformations. In addition, the level of internal stresses is also lower if compared with that following the application of, for instance, surfacing technologies. Sprayed layers have the lamellar structure characterised by various concertation of pores (of up to 20%). The thickness of sprayed layers tends to be greater than that of the layers obtained using other coating techniques and is usually restricted within the range of 0.05 mm to 2.0 mm [2]. Because of their internal stresses, it is assumed that the ultimate thickness of thermally sprayed layers should amount to 0.5 mm. The possibility of exceeding the above-named value should be confirmed in tests concerning a given spraying method, the pair of base materials and the coating. The manner in which the deposited

Dr inż. Marek St. Węglowski, dr inż. Robert Jachym, dr inż. Krzysztof Krasnowski, mgr inż. Krzysztof Kwieciński, dr inż. Janusz Pikuła, mgr inż. Piotr Śliwiński – Sieć Badawcza Łukasiewicz /Łukasiewicz Research Network - Instytut Spawalnictwa/

BY-NC

layer is joined with the substrate is of adhesive and mechanical nature. For this reason, thermally sprayed layers are characterised by lower adhesion (to the substrate) than those made using other technologies, e.g. involving the melting of the substrate surface (surfacing, alloying or melting).

Well-known and commonly used thermal spraying methods include the following:

- classical or infrasonic flame spraying,
- supersonic flame spraying (HVOF and HP/HVOF – *High Velocity Oxy Fuel*),
- arc spraying,
- plasma spraying,
- flame detonation spraying.

Table 1 presents the comparison of the most popular thermal spraying methods. The analysis takes into consideration the source of heat, the type of propellant (carrier gas), the form of sprayed material, the velocity of particles, types of sprayed materials, porosity and process efficiency.

Thermally sprayed layers can be used as [3]:

- abrasive wear resistant layers,
- thermal insulation,
- corrosion resistant layers,
- electric conductors or insulators,
- friction sealing surfaces,
- refurbished layers,
- special property layers (e.g. catalysts, active or passive surfaces,
- medical implants,
- special applications.

Some disadvantages of the spraying process, for instance the relatively high porosity or low adhesion of the sprayed layer, must be eliminated by the melting of the layer using the induction, arc, laser or electron beam-based method. Figure 1 presents the primary application areas of thermally sprayed layers.

Fig. 1. Primary application areas of thermally sprayed layers [7]

Table 1. Comparison of thermal spraying methods [2–5]

Method	Heat source	Carrier gas	Form of sprayed material	Heat source temperature [°C]	Velocity of particles striking the surface [m/s]	Type of sprayed material	Adhesion	Porosity [%]	Process efficiency [kg/hour]
arc	electric arc	air	wire	6000	240	metals	good	8–15	30
plasma	plasma electric arc	inert gas	powder	16000	120–600	metals, ceramics, plastics	very good	2–5	1–25
flame	oxy-acetylene flame	air	powder/ wire	3000	30–120	metals, ceramics,	poor	10–20	7–9
flame detonation	oxy-acetylene flame; additionally nitrogen, argon or oxygen	gas mixture	powder	4500	800	metals, ceramics, plastics	excellent	0.1–1	5
supersonic with high velocity (HVOF)	propylene/hydrogen/ propane/ acetylene, oxygen	air	powder/ wire	3000	800	metals, ceramics,	excellent	0.1–2	14

cc BY-NC

The authors of publication [6] presented an idea where sprayed layers are melted using the induction method, electric arc (in the TIG method) or plasma arc. In this article, the analysis of reference publications is concerned with the melting process involving the use of the concentrated electron beam.

Electron beam melting

Method

The concentrated electron beam is used in welding, surfacing, surface hardening and surface processing. The technology is characterised by significant technical and technological possibilities of controlling process parameters as regards the melting of sprayed layers. The heating and fast cooling in controlled conditions makes it possible to control microstructural transformations in the sprayed layer and in the base material. The modification performed The pulsed or continuous electron beam enables the modification of elements characterised by various porosity and shape. It is important that the surface subjected to processing should be perpendicular (as much as possible) to the electron beam. It is also possible to melt surfaces not perpendicular to the electron beam axis, provided that deflection is restricted within the range of several to less than twenty degrees.

The primary advantages of electron beam-based technologies are the following:
– different manner of heating and melting materials in comparison with the laser beam, enabling the faster heating of the material than through the conduction of heat,
– possibility of melting surfaces difficult to melt using other methods,
– melting process purity,
– limited distortions and changes in dimensions of elements subjected to processing,
– precise computer-aided beam control,
– precise adjustment of melting parameters,
– possibility of processing fragments of surfaces,
– high process repeatability,
– easy automation,
– high process precision (tolerances in micrometres),
– high efficiency,
– very low energy consumption (power efficiency of up to 80–90%).

Electron beam melting can be used with many materials. One of the limitations is concerned with materials containing zinc as an alloying element (characterised by low vapour pressure). In addition, the melting of duplex steels can be accompanied by the reduction of alloying elements in alloys, altering the phase equilibrium between the ferritic and austenitic phases (potentially reducing corrosion resistance). Nevertheless, electron beam melting constitutes an alternative to arc or laser beam-based methods.

The primary technological parameters of the electron beam melting process are the following:
– accelerating voltage, U [kV],
– electron beam current, I [mA],
– melting rate, v [mm/s], [cm/min],
– beam deflection frequency, f [Hz],
– focal length, [mm],
– type of oscillation,
– vacuum level, P [mbar].

Figure 2 presents the schematic diagram of the electron beam melting of the sprayed layer.

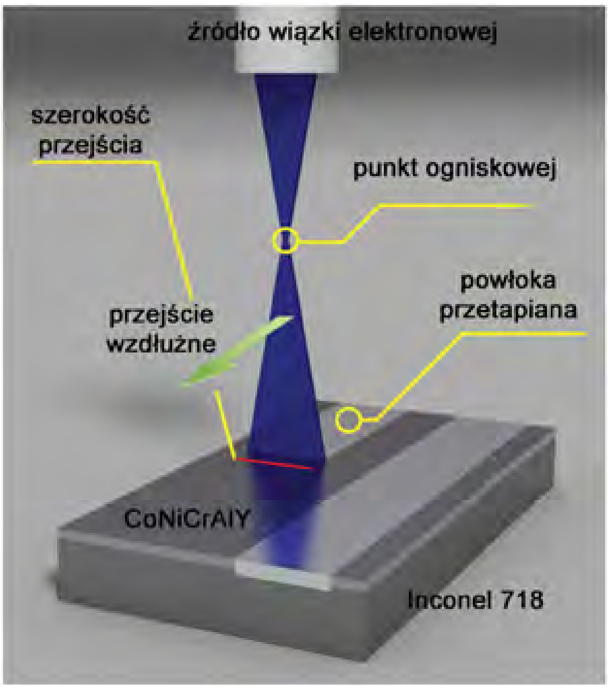

Fig. 2. Electron beam melting process

BY-NC

Application

Continuous casting moulds in continuous steel casting lines are made of copper, the surface of which is protected against wear with a galvanised nicker layer. Publication [8] presents tests results concerning the electron beam melting of a layer sprayed using the HVOF method, Stellite 6, self-fusible Ni alloy and WC-12Co (aimed to ultimately increase the service life of continuous casting moulds). Related tests revealed the favourable effect of the high frequency electron beam oscillation (Fig. 3), resulting in the reduction of porosity. The dynamic movement of the liquid metal pool was responsible for the release of gases. The melting also increased the adhesion of the layer to the substrate, the average value of which amounted to 350 MPa (before the melting process, the aforesaid value did not exceed 270 MPa).

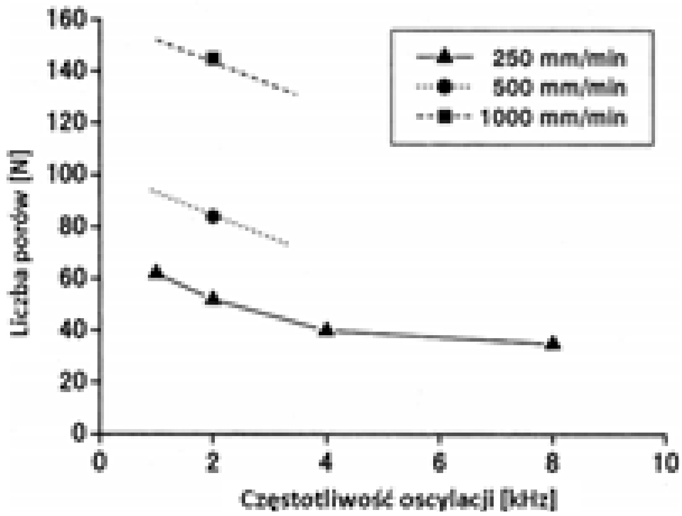

Fig. 3. Effect of high frequency electron beam oscillation on the porosity of melted layers [8]

The authors [9] presented test results concerning the electron beam melting of an HVOF-sprayed layer. The substrate (plate) made of copper (100 mm ×100 mm) was sprayed with powder (37.5% Co, 32% Ni, 22% Cr, 8% Al and 0.5% Y). The electron beam melting process was performed using the following technological parameters: U=30 kV, I=10–40 mA, v=3–17 mm/s and f=1 kHz. The tests revealed that the layer in the as-received state was characterised by a significant number of voids, non-uniform surface and numerous oxide areas. After melting, the surface of the sprayed layer was made even and its porosity was eliminated. Detailed metallographic tests revealed that, after melting, the layer was composed of two areas. The upper part was characterised by the lack of oxidised areas indicating that the layer had undergone refinement. In the lower part, the refinement process was not intense, thus leaving some oxide areas. The metallographic tests also revealed that an increase in electron beam current translated into the higher homogenisation of the microstructure and the increased thickness of the melted layer (particularly its upper part). It was also observed that an increase in the melting rate resulted in the porosity of the layer. The authors also demonstrated that the melting of the sprayed layer improved its corrosion resistance in comparison with that of the layer in the as-received state.

The electron beam melting process is also very useful to improve the quality of layers obtained using the cold spraying method. Authors [10] performed comparative tests concerning the melting of HVOF-sprayed and cold sprayed layers (using powder CoNiCrAlY: 0.98% C, 0.74% O, 6.16% Al, 19.35% Cr, 36.91% Co, 34.38% Ni and 1.47% Y). Layers were sprayed onto a substrate made of nickel alloy 718. In both cases it was possible to observe the banded structure (characteristic of thermal spraying processes) and porosity. The electron beam melting process was performed using a beam current of 4.6 mA and 6.2 mA as well as a melting rate restricted within the range of 10 mm/s to 20 mm/s. Metallographic tests revealed that the layers subjected to melting were characterised by lower porosity and uniform microstructure. The phase composition of the melted layers was similar to that of the initial state (before melting). In addition, it was possible to identify such phases as AlCo, $AlYO_3$ and $Al_5Y_3O_{12}$ in relation to the HVOF method as well as AlCo, Al_2O_3 and FeNi in relation to the layer obtained using the cold spraying method.

BY-NC

The electron beam melting of plasma sprayed layers increased their nanohardness. Publication [11] presents test results concerning the electron beam melting of sprayed layers, where powder PGAN-33 (22–24% Cr, 4% Mo, 2% Si, 1–1.5% W, 2% B and bal. Ni) was deposited on the substrate of unalloyed steel. As a result of the process, the nanohardness of the surface increased to 320 kg/mm^2. In addition, the adhesion of the layer increased from 57 MPa to 192 MPa, whereas its abrasive wear resistance increased twenty times.

Publication [12] presents results of tests involving the electron beam melting of plasma sprayed layers, where powder ZrO_2 + 7% Y_2O_3 was deposited on the substrate of corrosion resistant steel. The melting was performed using the following technological parameters: U=30 kV, I=0.33 mA and a scanning time of 200 ms. Figure 4 presents metallographic test results concerning the layers before and after the melting process. The tests revealed that the melting of the thermally sprayed layers increased their hardness both on the surface and in cross section (Fig. 5). In addition, the melting process significantly improved their abrasive wear resistance (Fig. 6).

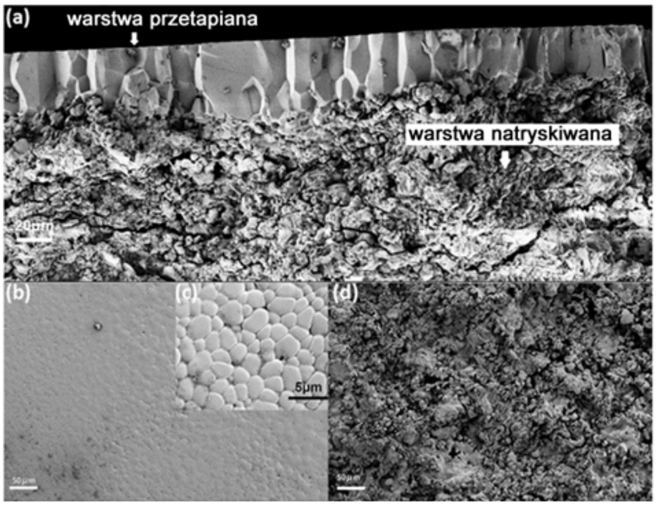

Fig. 4. Results of the metallographic tests of: a) layer after melting, b) layer after melting– surface and c) layer before melting – surface [12]

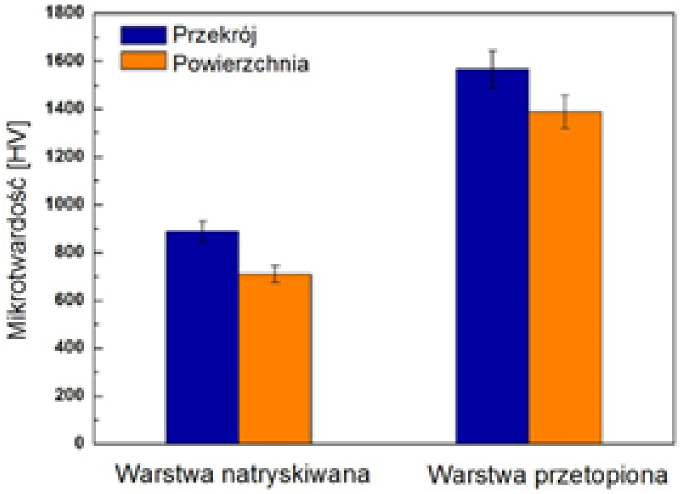

Fig. 5. Hardness of the thermally sprayed layer and melted layer [12]

The authors of publication [13] presented test results concerned with the electron beam melting of a layer made through the sintering of powder Ti-Cr-Si and sprayed onto the surface of alloy Nb+10%W. The electron beam melting process was performed using the following parameters U=40 kV, I=17 mA, v=570 mm/min and f 200 Hz. The melting process led to the significant refinement of the grain (Fig. 7) from 19 µm to 2 µm and to the obtainment of the $NbSi_2$ phase doped with Ti and Cr (68% Nb, 8% Si and 2% Ti, Cr).

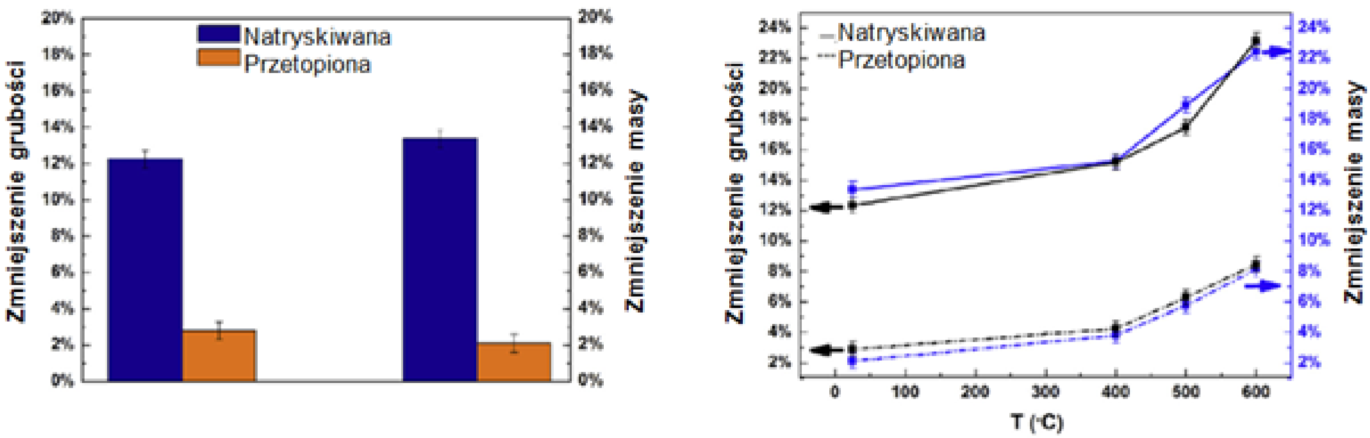

Fig. 6. Effect of the electron beam melting of the thermally sprayed layer on its abrasive wear resistance: a) at room temperature and b) in relation to temperature [12]

BY-NC

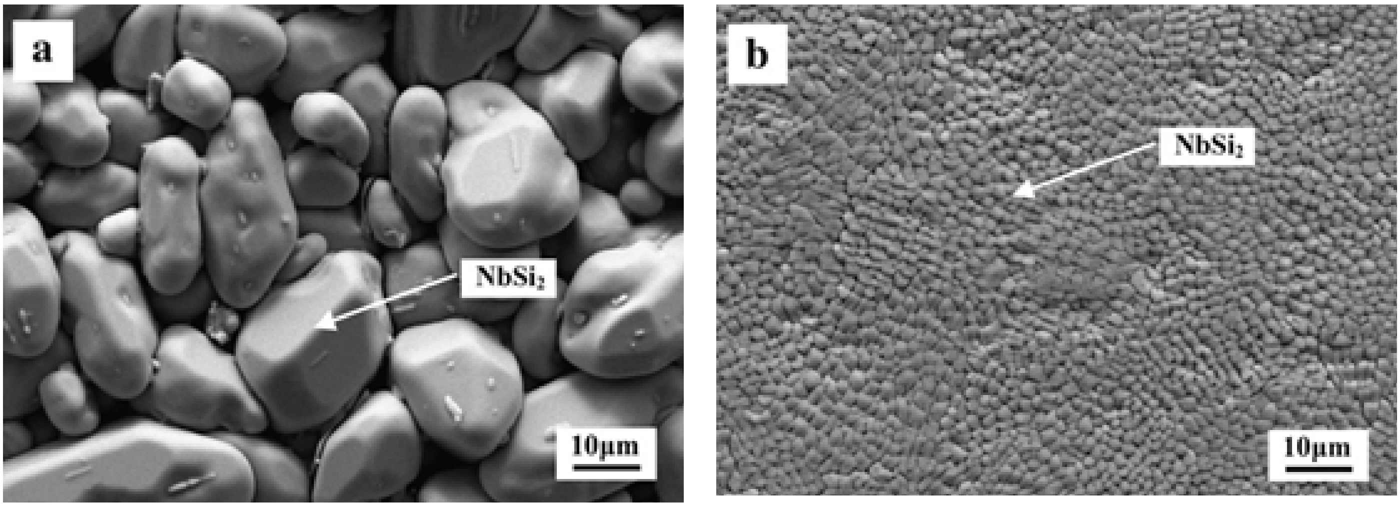

Fig. 7. Microstructure of the sprayed and sintered powder: a) before electron beam melting and b) after the melting process [13]

The surface roughness decreased from 10 µm to 0.1 µm, whereas resistance to oxidation at elevated temperature improved. The research included the performance of tests aimed to identify resistance to isothermal oxidation at a temperature of 1700°C. The hold time amounted to 40 hours in relation to the surface not subjected to melting and 50 hours in relation to the surface subjected to the melting process.

Publication [14] presents the effect of electron beam melting on the characteristics of a thermal oxide layer formed during oxidation in air at a temperature 950°C on an HVOF-sprayed MCrAlY layer. The layer (Co–32Ni–22Cr–8Al–0.5Y) was made on the substrate of alloy Inconel 716. The tests revealed that the electron beam melting of the MCrAlY layer before the EBPVD deposition of the ZrO_2 surface layer led to an increase in the oxide layer during oxidation in air at a temperature of 950°C. The melting process resulted in the obtainment of a thermal barrier coating (TBC). The electron beam melting process reduced the content of oxides and the porosity of thermally sprayed MCrAlY layers. The surface was melted to a depth of approximately 30 µm. High cooling rates made it possible to modify the morphology and the phase composition of the MCrAlY layer as well as to improve its adhesion to the substrate.

Work [15] discusses in more detail the effect of electron beam melting on the oxidation of layers. The publication presents test results concerning an electron beam melted HVOF-sprayed layer, where powder (37.5% Co, 32% Ni, 22% Cr, 8% Al and 0.5 % Y) was deposited on the substrate of alloy Inconel 617. After electron beam melting, the CoNiCrAlY layer was characterised by the refined microstructure, resulting from the rate of crystallisation. The layer did not contain pores or oxides. In addition, the melting process reduced roughness of the layer surface. It was possible to observe the cellular microstructure with phase β-AlNi in matrix γ Ni/γ'- $AlNi_3$. The X-ray analysis also confirmed the presence of the two phases in the microstructure of the layer subjected to electron beam melting. The melting process also affected the oxidation of the layer at high temperatures. During tests performed for 168 hours at a temperature of 950°C, the post-treatment smooth surface and refined microstructure free from pores and internal oxides facilitated the formation of the uniform and compact layer of oxides adhesive to the surface.

Publication [16] presents test results concerning the electron beam melting of an HVOF-sprayed layer, where powder 86% WC + 10% Co+4% Cr was deposited on the substrate of alloy Inconel 617. The tests revealed that the melting process increased the hardness of the layer

BY-NC

from 905 HV0.3 to 1100 HV0.3 (base material hardness amounted to 495 HV0.3). After the melting process, the abrasive wear resistance of the layer decreased slightly (Fig. 8), yet its resistance to corrosion in seawater increased. The density of current in terms of the melted layer amounted to 2.34 μA/cm². In turn, the density of current as regards the layer not subjected to melting amounted to 13.45 μA/cm² (in relation to nickel alloy Inconel 617, the aforesaid value amounted to 1.99 μA/cm²). The XRD analysis revealed that the melting process led to the formation of new phases, i.e. particularly Cr9Mo21Ni20 as well as phases doped with σ-CoCr. Both of the above-named phases increased the resistance of the material to corrosion in seawater.

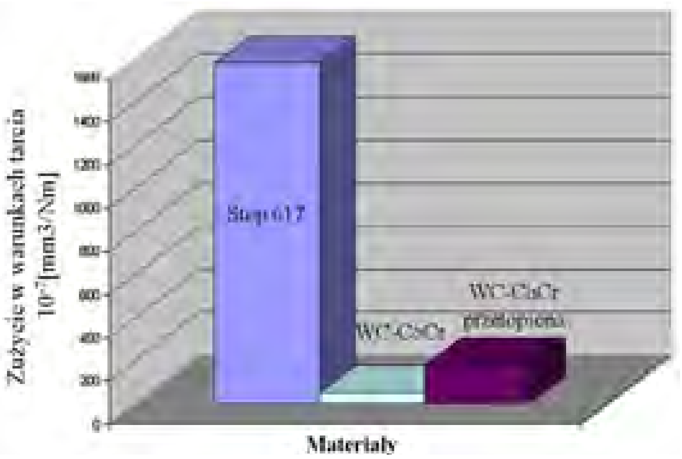

Fig. 8. Abrasive wear resistance of alloy 617, HVOF-sprayed WC-CoCr layer and the layer subjected to electron beam melting [16]

Publication [17] presents tests results related to the melting of a thermally sprayed material subjected to plasma nitriding (leading to the hardening of the material surface). The deposited material was powder having the following composition 15.8% Si, 5.1% Fe, 2.6% Cu, 0.5% Mg and Al – balance. The microstructure of the alloy consisted of the α-Al solid solution, Sip precipitates as well as the Al_7Cu_2Fe and $Al_9Fe_2Si_2$ intermetallic phases. The hardness of the base material amounted to 108 HV0.1. The plasma nitriding process did not increase the hardness of the material surface, yet it significantly improved the abrasive wear resistance of the material (Fig. 9). Further abrasive wear resistance was obtained after electron beam melting (Fig. 9). In addition, the hardness of the sprayed material rose to 200 HV0.1.

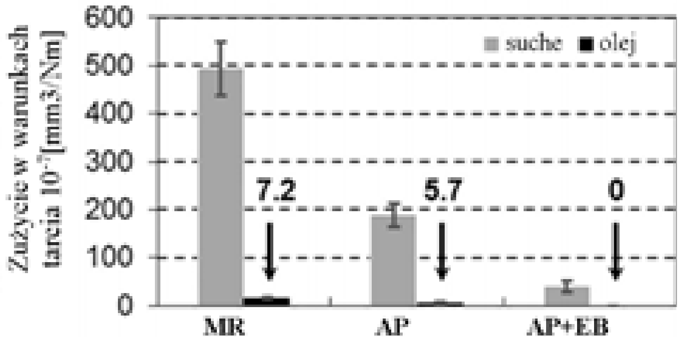

Fig. 9. Abrasive wear resistance of: base material – BM, after plasma nitriding– PN and electron beam melting – EB, in a watery and oily environment [17]

The comparison of the XRD patterns revealed that the electron beam melting process resulted in the formation of a new phase, i.e. Al_3FeSi_2 (δ-AlFeSi) in the layer, whereas the $Al_9Fe_2Si_2$ (β-AlFeSi) and Al_7Cu_2Fe (present in the base material) dissolved. In addition, measurements in the melted material revealed that the greatest distortions were present at the edge of the fusion zone and amounted to approximately 10 μm (Fig. 10).

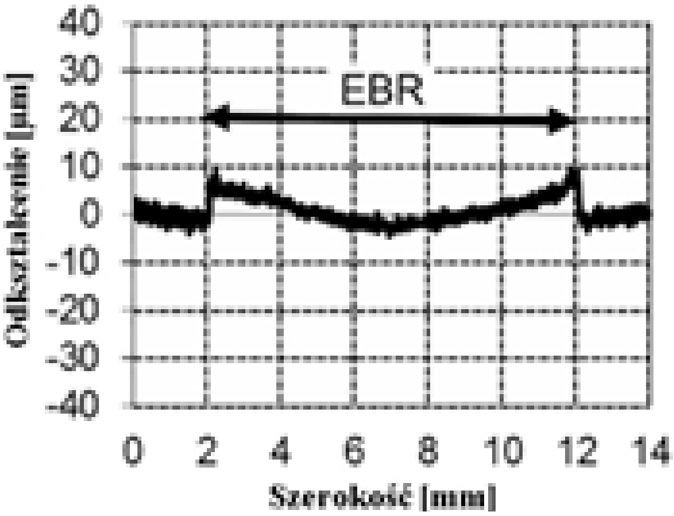

Fig. 10. Electron beam melting effect on surface deformation [17]

In work [18], the authors demonstrated the effect of electron beam melting parameters on the level of stresses in the material and on the properties of obtained layers. An $NbSi_2$ layer

cc BY-NC

was made on the substrate of the Nb + 10% W alloy using the stir-casting method. Afterwards, for 30 minutes, the layer was subjected to sintering at a temperature of 1350°C and under a pressure of 0.1 Pa. The layer obtained in the above-presented manner was then subjected to the electron beam melting process performed using the following technological parameters: U=30; 35; 40; 45 kV, I=18 mA, Io=1680 mA, v=480 mm/min and f=150 Hz.

The results of residual stress measurements are presented in Figure 11. Stresses generated in the $NbSi_2$ layer (not subjected to melting) amounted to approximately 50 MPa. After electron beam melting, a significant residual tensile stress of approximately 400 MPa was present in relation to an accelerating voltage of 30 kV. Afterwards, the stress level decreased to 270 MPa in relation to 35 kV. It should be noted that in relation to an accelerating voltage of 40 kV, tensile stress transformed into compressive one. The above-named phenomenon was explained by the authors as presented below. When voltage amounted to 35 kV, the melted material particles in the layer were characterised by the fast crystallised surface, which was connected with volume shrinkage. The lower (non-melted) layer was responsible for the hardening of the upper layer, which, in turn, led to the generation of tensile stresses. The foregoing led to the formation of surface cracks (see Figure 12a). However, when voltage amounted to 40 kV, because of the greater layer penetration depth and a relatively high gradient of temperature, the upper surface cooled without volume shrinkage, yet the subsurface area contracted. The foregoing resulted in the formation of compressive stresses on the layer surface. The aforesaid compressive stresses and the greater penetration depth were responsible for the reduced number of cracks and pores. Asa result, the obtained layer was free from imperfections (Fig. 12b).

Figure 13 presents measurement results concerning the hardness of the $NbSi_2$ surface before and after electron beam melting. The hardness of the layer before the melting process amounted to approximately 300 HV0.5. An increase in accelerating voltage was accompanied by an increase in the hardness of the layer, resulting from the refinement of the microstructure. A further increase in hardness observed in relation to voltage over 35 kV was also triggered by the reduction of residual tensile stresses (Fig. 11) and the reduction of porosity.

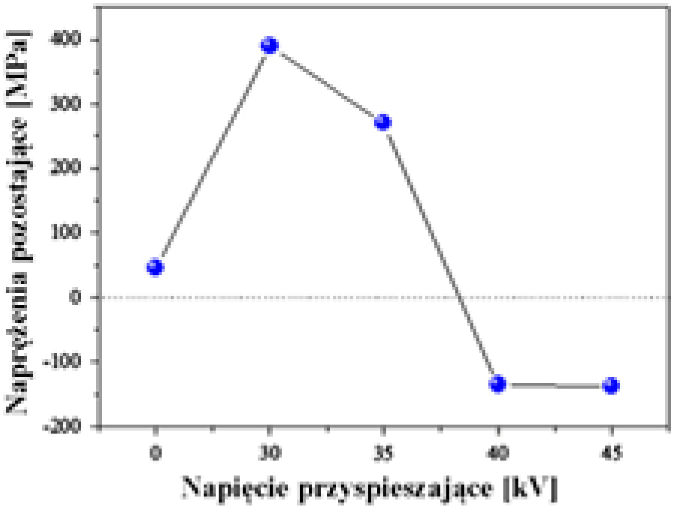

Fig. 11. Effect of accelerating voltage on residual stresses after electron beam melting [18]

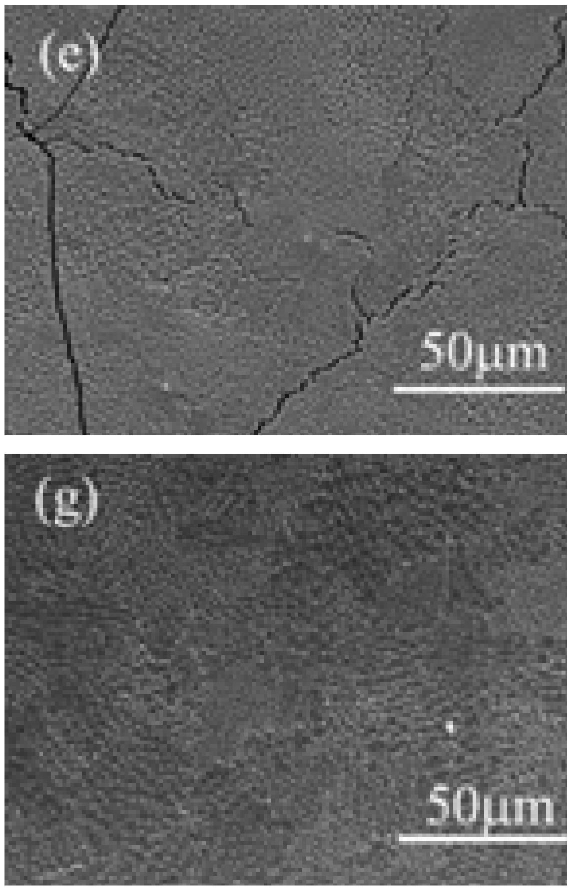

Fig. 12. Microstructure (SEM) of the NbSi2 layer subjected to electron beam melting: a) U=30 kV and b) U=40 kV [18]

BY-NC

A voltage of 40 kV was accompanied by the presence of compressive stresses in the layer, which translated into a further increase in hardness. When voltage amounted to 45 kV, in addition to the presence of residual compressive stresses, the microstructure was also characterised by the presence of the Nb5Si3 phase. The above-named phrase was characterised by a high melting point and hardness, which, in turn, translated into the highest hardness of the layer after melting.

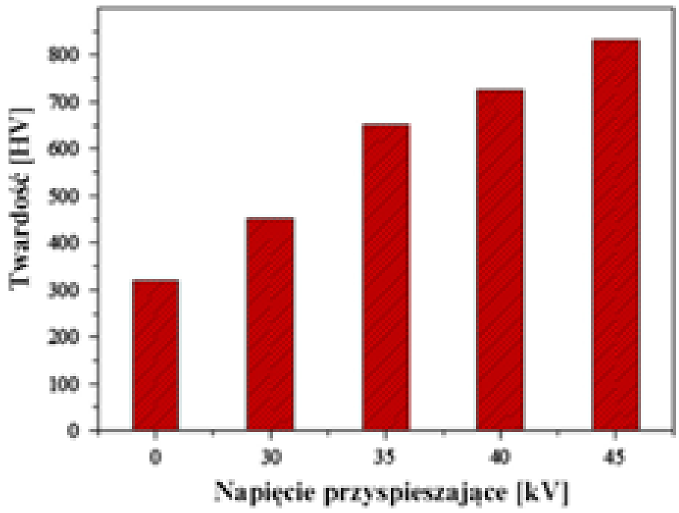

Fig. 13. Effect of accelerating voltage on the hardness of layers subjected to electron beam melting [18]

Publication [19] presents test results concerning the electron beam melting of an HVOF-sprayed Al_2O_3+TiO_2 layer deposited on the substrate od technical titanium. As a result of the melting process, the hardness of the layer increased from 960 HV0.3 to 1825 HV0.3 (base

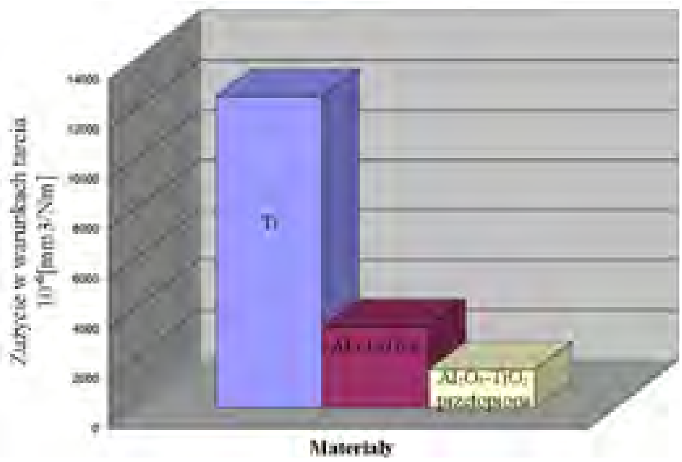

Fig. 14. Electron beam melting effect on abrasive wear resistance [19]

material hardness amounted to 370 HV0.3). The use of the electron beam melting process also improved the abrasive wear resistance of the layer (Fig. 14).

The melting process also increased corrosion resistance in the solution of NaCl. The density of current in terms of the melted layer amounted to 55.7 nA/cm². In turn, the density of current as regards the layer not subjected to melting amounted to 216.1 nA/cm² (in relation to titanium, the aforesaid value amounted to 10.5 nA/cm²). The melted layer was characterised by greater density and microstructural homogeneity. The process enabled the elimination of pores, voids and lamellar structure.

The comparative test results concerning two spraying technologies are presented in publication [20]. The substrate of alloy Inconel 718 was provided with layers made of the CoNiCrAlY powder (Diamalloy 4700, HC Starck, Germany) deposited using the HVOF method and the cold spraying method. The melting was performed using the following technological parameters: U=120 kV, I=3–18 mA, v=15 and 20 mm/s. Table 2 presents test results concerning sprayed and melted layers.

The electron beam melting process enabled the obtainment of the homogenous microstructure both as regards the cold sprayed and HVOF-sprayed layers. In addition, the process made it possible to reduce the porosity of the material surface and its roughness as well as to increase the hardness of the layer (in comparison with its hardness directly after spraying).

Publication [21] presents test results concerning sprayed layers deposited on the substrate of magnesium alloys AZ91, AZ31 and AM20 and subjected to the electron beam melting process performed using the following parameters: U=60–80 kV, pressure in the chamber: 10–4 – 10– 5 kPa, I=5–25 mA and v=5–30 mm/s. Sprayed materials were alloy powders obtained through mechanical mixing and characterised by various contents of hard particles and aluminium. Flux-cored wires were made

cc BY-NC

Table 2. Properties of the sprayed layers subjected to electron beam melting [20]

Method	Layer thickness [μm]	Young's modulus [GPa]	Hardness [GPa]	Porosity [%]	Roughness *Ra* [μm]
CS-A	756	8008±285	171±14	0.13	11.7
CS-B	1197	5114±239	190±5	0.05	2.7
CS-C	924	5416±266	206±6	0.02	2.1
HVOF-A	40	8175±325	174±8	5.81	6.1
HVOF-B	37	6821±434	184±11	4.15	5.7
HVOF-C	43	4641±57	186±7	1.67	3.5
CS-A cold spraying before melting, CS-B, EB melting, I=14 mA, v=15 mm/s, CS-C EB melting, I=18 mA, v=20 mm/s, HVOF-A – before melting, HVOF-B EB melting, I=3 mA, v=20 mm/s, HVOF-C EB melting, I=4 mA, v=20 mm/s					

of aluminium strips filled with hard particles. The tests also involved the use of solid zinc alloy wires. The HVOF spraying process involved the use of alloy powders Al_2O_3, Cr_2O_3 and TiO_2 and pure aluminium as the matrix. The tests also involved the use of mechanically mixed powder Al12Si and TiO_2 (50:50 vol%). The mechanically mixed Al/SiC powder (50:50 vol%) was also used to make a vacuum plasma sprayed layer (VPS). Arc spraying was performed using aluminium wires having a diameter of 1.6 mm and filled with TiO_2, SiC, B_4C or FTC powders. The flux-cored wire filling coefficient amounted to 25 % by weight in relation to the Al/SiC wire, 30 % by weight in relation to the Al/B_4C wire, 20% by weight in relation to the Al/TiO_2 wire and 55 by weight in relation to the Al/FTC wire. Solid wires used in arc spraying had a diameter of 1.6 mm and were made of zinc-aluminium alloys ZnAl4 and ZnAl15.

As regards the Al/TiO_2 layers, depending on electron beam melting parameters, the melted layer was characterised by the redistribution of TiO_2 and $TiAl_3$ particles. In addition, it was possible to observe the formation of the Al_2TiO_5 oxide (Fig. 15).

The metallographic tests revealed that the microstructure was homogenous and the deposition of the hard particles in aluminium was satisfactory. It was also possible to observe a slight decrease in the concentration of the particles on the layer surface. The tests revealed that the melted arc sprayed layers obtained using the Al/TiO_2 wire (80:20vol%) contained particles of $TiAl_3$ (formed already during the arc spraying process) and a slight amount of secondary oxides Al_2TiO_5.

The VPS layers obtained using the mechanically mixed powders, i.e. Al/SiC and Al/Al_2O_3, were characterised by higher roughness

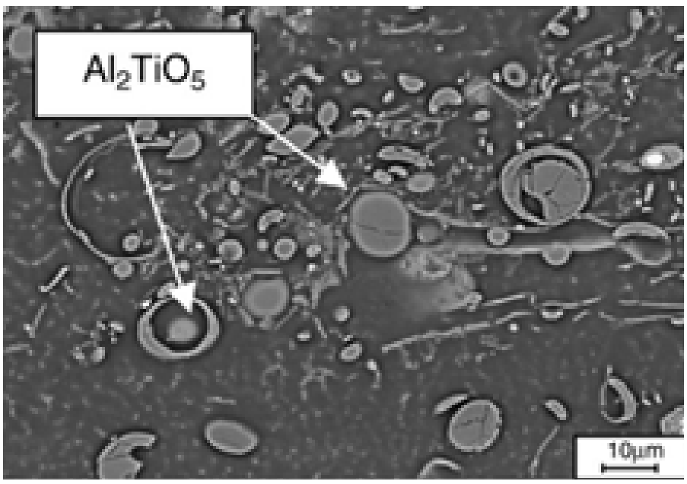

Fig. 15. Microstructure of the HVOF-sprayed Al/TiO_2 layer deposited on the substrate of alloy AZ91 [21]

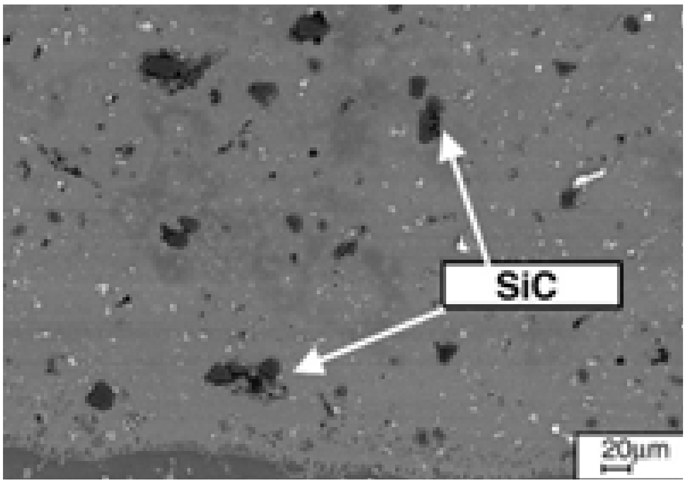

Fig. 16. Microstructure of the VPS Al/SiC layer (20:80 vol%) after electron beam melting [21]

BY-NC

in comparison with the HVOF-sprayed layers. As regards the Al/SiC layers (Fig. 16), the electron beam melting process enabled the obtainment of uniform distribution of carbides. At the same time, the above-named layers were characterised by the significant concentration of brittle Al_4C_3 carbides.

In the arc sprayed layers made using flux-cored wires containing tungsten carbide it was possible to observe the partial melting of carbides during the deposition of the layer (because of the high process temperature). The electron beam melting process was responsible for the solution of the non-melted carbides and the formation of a new phase, i.e. $Al_{12}Mg_{17}$. In spite of the significant density of FTC, its concentration in the melted layer was not uniform and decreased from the surface towards the substrate.

Summary

For many years, thermal spraying technologies have been used to make layers characterised by various properties (depending on application and operating conditions). However, the above-named layers are also characterised by porosity, lamellar microstructure, excessive roughness and, in cases of many applications, insufficient adhesion to the substrate. Some of the aforesaid disadvantages can be limited or even eliminated by the appropriate adjustment spraying process technological parameters, the changing of the material to be sprayed or by changing the of technology itself. Another possible solution involves the application of the additional treatment (melting) of the layer. Melting processes can involve the use of gas flame, arc, induction as well as the laser or electron beam. The electron beam melting process is a technology which can be applied successfully, especially due to the fact that it is performed under vacuum conditions, thus enabling the additional refinement of liquid material. The above-presented tests revealed that, in relation to a wide range of sprayed materials, spraying technologies and base materials, the electron beam melting of the layer makes it possible to eliminate or significantly limit porosity, homogenise the microstructure, reduce surface roughness as well to increase abrasive wear resistance and resistance to corrosion. In addition, short cooling rates lead to the significant refinement of the microstructure and an increase in layer hardness. Appropriately adjusted technological parameters also enable the obtainment of crack-free layers. The performance of the process under vacuum conditions prevents the formation of oxides layers.

Acknowledgements

The tests were performed within the project entitled *Layers and Coatings Containing Rhenium, its Compounds or Alloys – Properties, Application and Deposition Methods* (contract no. CuBR/II/4/2015) financed by the National Centre for Research and Development (Narodowe Centrum Badań i Rozwoju) and KGHM Polska Miedź S.A.

References

[1] https://www.marketsandmarkets.com/Market-Reports/thermal-spray-coating-market-181347083.html?gclid=CjwKCAjwu5CDBhB9EiwAow6sLUl1pADDJCB5U8lQcUC_QvxViA3_mOdfYXOe3QneAI5qUOelX7d-KhoCO68QAvD_BwE.

[2] Dobrzański L.A., Dobrzańska-Danikiewicz A.D.: Obróbka powierzchni materiałów inżynierskich. International OCSCO World Press, Gliwice 2011.

[3] Adamiec P., Dziubiński J.: Wytwarzanie i właściwości warstw wierzchnich elementów maszyn transportowych. Wydawnictwo Politechniki Śląskiej, Gliwice 2005.

[4] Studies on the properties of high-velocity oxy–fuel thermal spray coatings for higher temperature applications. Materials Science, 2005, vol. 41, no. 6, pp. 805–823.

BY-NC

https://doi.org/10.1007/s11003-006-0047-z .
[5] Ulianitsky V.Y., Dudina D.V. i in.: Computer-Controlled Detonation Spraying: FlexibleControl of the Coating Chemistry and Microstructure. Metals, 2019, vol. 9, 1244. doi:10.3390/met9121244.
[6] Węglowski M.St., Jachym R., Krasnowski K., Kwieciński K., Pikuła J.: Przetapianie indukcyjne i łukiem elektrycznym warstw natryskiwanych cieplnie – przegląd zagadnienia. Biuletyn Instytutu Spawalnictwa, 2021, vol. 65, no. 1, pp. 7–16.
[7] Ghadami F., Sabour Rouh Aghdam A.: Improvement of high velocity oxy-fuel spray coatings by thermal posttreatments: A critical review. Thin Solid Films, 2019, vol. 678, pp. 42–52. https://doi.org/10.1016/j.tsf.2019.02.019.
[8] Hamatani H., Miyazaki Y.: Optimization of an electron beam remelting of HVOF sprayed alloys and carbides. Surface and Coatings Technology, 2002, vol. 154, pp. 176–183. https://doi.org/10.1016/s0257-8972(01)01713-3.
[9] Utu D., Brandl W. et al.: Morphology and phase modification of HVOF-sprayed MCrAlY-coatings remelted by electron beam irradiation. Vacuum, 2005, vol. 77, pp. 451–455. https://doi.org/10.1016/j.vacuum.2004.09.006.
[10] Gavendová P., Čížek J. et al.: Microstructure modification of CGDS and HVOF sprayed CoNiCrAlY bond coat remelted by electron beam. Procedia Materials Science, 2016, vol. 12, pp. 89 – 94. https://doi.org/10.1016/j.mspro.2016.03.016.
[11] Pogrebnjak A.D., Ruzimov Sh. M., Alontseva D.L., Żukowski P., Karwat C., Kozak C., Kolasik M.: Structure and properties of coatings on Ni base deposited using a plasma jet before and after electron a beam irradiation. Vacuum, 2007, vol. 81, pp. 1243–1251. https://doi.org/10.1016/j.vacuum.2007.01.071.
[12] Wu Y.Z., Liao W.B. et al.: Effect of electron beam remelting treatments on the performances of plasma sprayed zirconia coatings. Journal of Alloys and Compounds, 2018, vol. 756, pp. 33–39. https://doi.org/10.1016/j.jallcom.2018.05.004.
[13] He J., Zhang B. et al.: Morphology of sintered silicide coatings remelted by high frequency electron beam. Surface & Coatings Technology, 2012, vol. 209, pp. 52–57. https://doi.org/10.1016/j.surfcoat.2012.08.027
[14] Utu D., Marginean G. et al.: Improvement of the oxidation behaviour of electron beam remelted MCrAlY coatings. Solid State Sciences, 2005, vol. 7, pp. 459–464. https://doi.org/10.1016/j.solidstatesciences.2005.01.003.
[15] Marginean G., Frunzaverde D. et al.: Influence of Electron Beam and Laser Remelting on the Oxidation Behaviour of HVOF-sprayed CoNiCrAlYCoatings. Berg Huettenmaenn Monatsh, 2007, vol. 152, pp. 32–38. https://doi.org/10.1007/s00501-006-0269-2.
[16] Marginean G., Utu D.: Microstructure refinement and alloying of WC–CoCr coatings by electron beam treatment. Surface & Coatings Technology, 2010, vol. 205, pp. 1985–1989. https://doi.org/10.1016/j.surfcoat.2010.08.095.
[17] Jung A., Buchwalder A.: Surface engineering of spray-formed aluminium-silicon alloys by plasma nitriding and subsequent electron beam remelting. Surface & Coatings Technology, 2018, vol. 335, pp. 166–172. https://doi.org/10.1016/j.surfcoat.2017.12.016.
[18] He J., Zhang B.G., Li W.L.: The dependence of the electron beam remelting parameters on the surface residual stress and hardness of NbSi2 coatings on niobium alloys. Journal of Alloys and Compounds, 2013, vol. 577, pp. 436–438. https://doi.org/10.1016/j.jallcom.2013.06.120.
[19] Utu I.D., Marginean G.: Effect of electron

BY-NC

beam remelting on the characteristics of HVOF sprayed Al2O3-TiO2 coatings deposited on titanium substrate. Colloids and Surfaces A: Physicochemical and Engineering Aspects, 2017, vol. 526, pp. 70–75. https://doi.org/10.1016/j.colsurfa.2016.10.034.

[20] Cizek J., Matejkova M. et al.: Potential of New-Generation Electron Beam Technology in Interface Modification of Cold and HVOF Sprayed MCrAlY Bond Coats. Advances in Materials Science and Engineering, 2016, Article ID 9070468, p. 6 http://dx.doi.org/10.1155/2016/9070468.

[21] Pokhmurska H., Wielage B. et al.: Post-treatment of thermal spray coatings on magnesium. Surface & Coatings Technology, 2008, vol. 202 , pp. 4515–4524. https://doi.org/10.1016/j.surfcoat.2008.04.036.